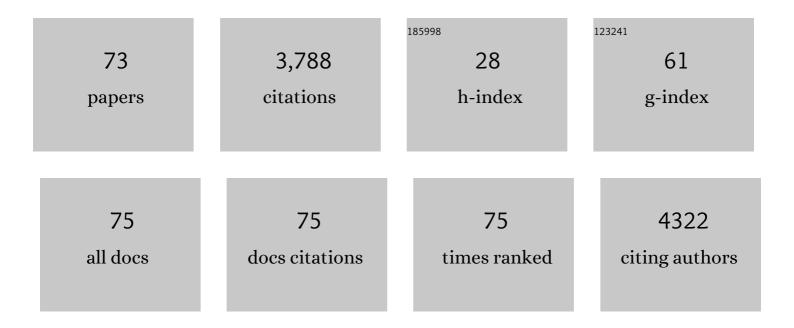
## Xue-Zhi Song

List of Publications by Year in descending order

Source: https://exaly.com/author-pdf/2190667/publications.pdf Version: 2024-02-01



XUE-7HI SONC

#	Article	IF	CITATIONS
1	Singleâ€Crystalâ€toâ€Singleâ€Crystal Transformation of a Europium(III) Metal–Organic Framework Producing a Multiâ€responsive Luminescent Sensor. Advanced Functional Materials, 2014, 24, 4034-4041.	7.8	542
2	One-dimensional channel-structured Eu-MOF for sensing small organic molecules and Cu2+ ion. Journal of Materials Chemistry A, 2013, 1, 11043.	5.2	341
3	Highly efficient heterogeneous catalytic materials derived from metal-organic framework supports/precursors. Coordination Chemistry Reviews, 2017, 337, 80-96.	9.5	282
4	Titanium Dioxide: From Engineering to Applications. Catalysts, 2019, 9, 191.	1.6	277
5	Lanthanide Ion Codoped Emitters for Tailoring Emission Trajectory and Temperature Sensing. Advanced Functional Materials, 2015, 25, 1463-1469.	7.8	263
6	A Metal–Organic Framework/DNA Hybrid System as a Novel Fluorescent Biosensor for Mercury(II) Ion Detection. Chemistry - A European Journal, 2016, 22, 477-480.	1.7	155
7	A europium( <scp>iii</scp> ) based metal–organic framework: bifunctional properties related to sensing and electronic conductivity. Journal of Materials Chemistry A, 2014, 2, 237-244.	5.2	149
8	Encapsulation of Ln <sup>III</sup> Ions/Dyes within a Microporous Anionic MOF by Postâ€synthetic Ionic Exchange Serving as a Ln <sup>III</sup> Ion Probe and Twoâ€Color Luminescent Sensors. Chemistry - A European Journal, 2015, 21, 9748-9752.	1.7	123
9	Prussian Blue analogue derived porous NiFe2O4 nanocubes for low-concentration acetone sensing at low working temperature. Chemical Engineering Journal, 2018, 338, 504-512.	6.6	116
10	Triple-shelled ZnO/ZnFe2O4 heterojunctional hollow microspheres derived from Prussian Blue analogue as high-performance acetone sensors. Sensors and Actuators B: Chemical, 2018, 256, 374-382.	4.0	96
11	A Temperatureâ€Responsive Smart Europium Metalâ€Organic Framework Switch for Reversible Capture and Release of Intrinsic Eu <sup>3+</sup> Ions. Advanced Science, 2015, 2, 1500012.	5.6	83
12	Prussian Blue Analogs and Their Derived Nanomaterials for Electrochemical Energy Storage and Electrocatalysis. Small Methods, 2021, 5, e2001000.	4.6	81
13	Hollow core–shell NiCo <sub>2</sub> S <sub>4</sub> @MoS <sub>2</sub> dodecahedrons with enhanced performance for supercapacitors and hydrogen evolution reaction. New Journal of Chemistry, 2019, 43, 3601-3608.	1.4	70
14	A Eu/Tb-codoped coordination polymer luminescent thermometer. Inorganic Chemistry Frontiers, 2014, 1, 757-760.	3.0	63
15	Syntheses, structures and physical properties of transition metal–organic frameworks assembled from trigonal heterofunctional ligands. Dalton Transactions, 2012, 41, 10412.	1.6	58
16	Hollow NiFe <sub>2</sub> O <sub>4</sub> microspindles derived from Ni/Fe bimetallic MOFs for highly sensitive acetone sensing at low operating temperatures. Inorganic Chemistry Frontiers, 2018, 5, 1107-1114.	3.0	55
17	A Series of Metal–Organic Frameworks Constructed From a V-shaped Tripodal Carboxylate Ligand: Syntheses, Structures, Photoluminescent, and Magnetic Properties. Crystal Growth and Design, 2013, 13, 2756-2765.	1.4	52
18	Highly thermostable lanthanide metal–organic frameworks exhibiting unique selectivity for nitro explosives. RSC Advances, 2015, 5, 93-98.	1.7	46

XUE-ZHI SONG

#	Article	IF	CITATIONS
19	Concave ZnFe <sub>2</sub> O <sub>4</sub> Hollow Octahedral Nanocages Derived from Fe-Doped MOF-5 for High-Performance Acetone Sensing at Low-Energy Consumption. Inorganic Chemistry, 2017, 56, 13646-13650.	1.9	46
20	Recent Advances of CeO <sub>2</sub> â€Based Electrocatalysts for Oxygen and Hydrogen Evolution as well as Nitrogen Reduction. ChemElectroChem, 2021, 8, 996-1020.	1.7	45
21	Boosting Hydrogen Evolution Electrocatalysis via Regulating the Electronic Structure in a Crystalline–Amorphous CoP/CeO <sub><i>x</i></sub> p–n Heterojunction. ACS Applied Materials & Interfaces, 2022, 14, 33151-33160.	4.0	41
22	Hierarchical CuO@ZnCo–OH core-shell heterostructure on copper foam as three-dimensional binder-free electrodes for high performance asymmetric supercapacitors. Journal of Power Sources, 2020, 465, 228239.	4.0	40
23	Defect and interface engineering in metal sulfide catalysts for the electrocatalytic nitrogen reduction reaction: a review. Journal of Materials Chemistry A, 2022, 10, 6927-6949.	5.2	39
24	Carbon coated nickel–cobalt bimetallic sulfides hollow dodecahedrons for a supercapacitor with enhanced electrochemical performance. New Journal of Chemistry, 2018, 42, 5128-5134.	1.4	38
25	A series of POM/Ag-based hybrids: distinct forms and assembly of [AgxLy] complexes through combinational effects of POM and isomeric ligands. CrystEngComm, 2012, 14, 6452.	1.3	34
26	Two high-connected metal–organic frameworks based on d10-metal clusters: syntheses, structural topologies and luminescent properties. Dalton Transactions, 2013, 42, 8183.	1.6	32
27	Constructing porous MOF based on the assembly of layer framework and p-sulfonatocalix[4]arene nanocapsule with proton-conductive property. CrystEngComm, 2014, 16, 64-68.	1.3	31
28	Defect-engineered TiO2 Hollow Spiny Nanocubes for Phenol Degradation under Visible Light Irradiation. Scientific Reports, 2018, 8, 5904.	1.6	28
29	Heterostructural Co/CeO2/Co2P/CoP@NC dodecahedrons derived from CeO2-inserted zeolitic imidazolate framework-67 as efficient bifunctional electrocatalysts for overall water splitting. International Journal of Hydrogen Energy, 2020, 45, 30559-30570.	3.8	28
30	An unusual three-dimensional self-penetrating network derived from cross-linking of two-fold interpenetrating nets via ligand-unsupported Ag–Ag bonds: synthesis, structure, luminescence, and theoretical study. New Journal of Chemistry, 2012, 36, 877.	1.4	25
31	Hollow NiFe <sub>2</sub> O <sub>4</sub> hexagonal biyramids for high-performance <i>n</i> -propanol sensing at low temperature. New Journal of Chemistry, 2018, 42, 14071-14074.	1.4	25
32	<i>In situ</i> formation of defect-engineered N-doped TiO <sub>2</sub> porous mesocrystals for enhanced photo-degradation and PEC performance. Nanoscale Advances, 2019, 1, 1372-1379.	2.2	25
33	Employing tripodal carboxylate ligand to construct Co(ii) coordination networks modulated by N-donor ligands: syntheses, structures and magnetic properties. Dalton Transactions, 2013, 42, 13231.	1.6	24
34	SiO2-coated magnetic nano-Fe3O4 photosensitizer for synergistic tumour-targeted chemo-photothermal therapy. Colloids and Surfaces B: Biointerfaces, 2020, 195, 111274.	2.5	24
35	A facile photoassisted route to synthesis N, F-codoped oxygen-deficient TiO2 with enhanced photocatalytic performance under visible light irradiation. Applied Surface Science, 2018, 434, 725-734.	3.1	23
36	LnFeO3 (Ln La, Nd, Sm) derived from bimetallic organic frameworks for gas sensor. Journal of Alloys and Compounds, 2022, 902, 163803.	2.8	23

XUE-ZHI SONG

#	Article	IF	CITATIONS
37	Dual-stimuli-responsive TiO <sub>x</sub> /DOX nanodrug system for lung cancer synergistic therapy. RSC Advances, 2018, 8, 21975-21984.	1.7	21
38	Annealing temperature-dependent porous ZnFe2O4 olives derived from bimetallic organic frameworks for high-performance ethanol gas sensing. Materials Chemistry and Physics, 2020, 241, 122379.	2.0	21
39	Hollow CoP Encapsulated in an N-Doped Carbon Nanocage as an Efficient Bifunctional Electrocatalyst for Overall Water Splitting. ACS Applied Nano Materials, 2021, 4, 13450-13458.	2.4	20
40	Boosting the oxygen evolution electrocatalysis of high-entropy hydroxides by high-valence nickel species regulation. Chemical Communications, 2022, 58, 7682-7685.	2.2	20
41	Three three-dimensional anionic metal–organic frameworks with (4,8)-connected alb topology constructed from a semi-rigid ligand and polynuclear metal clusters. CrystEngComm, 2011, 13, 6057.	1.3	19
42	Three unprecedented open frameworks based on a pyridyl-carboxylate: synthesis, structures and properties. CrystEngComm, 2012, 14, 1681-1686.	1.3	19
43	Porous Javelinâ€Like NiFe <sub>2</sub> O <sub>4</sub> Nanorods as nâ€Propanol Sensor with Ultrahighâ€Performance. ChemistrySelect, 2018, 3, 12871-12877.	0.7	19
44	Spontaneously engineering heterogeneous interface of silver nanoparticles on α-Co(OH)2 for boosting electrochemical oxygen evolution. Journal of Alloys and Compounds, 2021, 873, 159766.	2.8	19
45	Seamless Interfacial Formation by Solution-Processed Amorphous Hydroxide Semiconductor for Highly Efficient Electron Transport. ACS Applied Energy Materials, 2018, 1, 4564-4571.	2.5	16
46	Double-shelled carbon nanocages grafted with carbon nanotubes embedding Co nanoparticles for enhanced hydrogen evolution electrocatalysis. Chemical Communications, 2021, 57, 3022-3025.	2.2	16
47	Direct Growth of Continuous and Uniform MoS <sub>2</sub> Film on SiO <sub>2</sub> /Si Substrate Catalyzed by Sodium Sulfate. Journal of Physical Chemistry Letters, 2020, 11, 1570-1577.	2.1	15
48	One-pot synthesis of oleic acid modified monodispersed mesoporous TiO2 nanospheres with enhanced visible light photocatalytic performance. Advanced Powder Technology, 2018, 29, 1925-1932.	2.0	14
49	Hierarchical MoO <sub>4</sub> <sup>2–</sup> Intercalating α-Co(OH) <sub>2</sub> Nanosheet Assemblies: Green Synthesis and Ultrafast Reconstruction for Boosting Electrochemical Oxygen Evolution. Energy & Fuels, 2021, 35, 2775-2784.	2.5	13
50	Synthesis of surfactantâ€modified ZIFâ€8 with controllable microstructures and their drug loading and sustained release behaviour. IET Nanobiotechnology, 2020, 14, 595-601.	1.9	12
51	Enhancing the Fe <sup>3+</sup> Sensing Sensitivity by Energy Transfer and Phase Transformation in a Bimetallic Lanthanide Metalâ€Organic Framework. ChemistrySelect, 2018, 3, 9564-9570.	0.7	11
52	Triple-shelled CuO/CeO <sub>2</sub> hollow nanospheres derived from metal–organic frameworks as highly efficient catalysts for CO oxidation. New Journal of Chemistry, 2019, 43, 16096-16102.	1.4	11
53	Interface Engineering and Phase Regulation in CoP/CePO <sub>4</sub> Heterostuctures for Boosting Oxygen Evolution Electrocatalysis. Energy & Fuels, 2021, 35, 16760-16767.	2.5	11
54	CeO2-modulated CoP derived from prussian blue analogue boosting hydrogen evolution reaction electrocatalysis. Journal of Alloys and Compounds, 2022, 913, 165334.	2.8	11

XUE-ZHI SONG

#	Article	IF	CITATIONS
55	A three dimensional N-doped graphene/CNTs/AC hybrid material for high-performance supercapacitors. RSC Advances, 2017, 7, 6664-6670.	1.7	9
56	A theoretical insight into CO2 sensing performance on the orthorhombic LaMnO3 (0 1 0) surface. Chemical Physics Letters, 2017, 687, 138-142.	1.2	8
57	High-Quality Inorganic Chemistry Teaching During COVID-19. Journal of Chemical Education, 2020, 97, 2945-2949.	1.1	7
58	Ammonium Salts: New Synergistic Additive for Chemical Vapor Deposition Growth of MoS <sub>2</sub> . Journal of Physical Chemistry Letters, 2021, 12, 12384-12390.	2.1	7
59	Interface Engineering in CoP/CePO <sub>4</sub> Derived from a Prussian Blue Analogue as a Highly Efficient Electrocatalyst for Alkaline Hydrogen Evolution Reaction. ChemElectroChem, 2021, 8, 3762-3766.	1.7	5
60	Hierarchical particle-on-sheet CoP fabricated by direct phosphorization of Co(OH)2/ZIF-67 hybrid for boosting hydrogen evolution electrocatalysis. Inorganic Chemistry Communication, 2021, 134, 109058.	1.8	5
61	Solution Effect on Synthesis of Polyaniline/rGO Composite for High-Performance Supercapacitor. Nano, 2017, 12, 1750088.	0.5	4
62	Synthesis of hollow donut-like carbon nitride for the visible light-driven highly efficient photocatalytic production of hydrogen and degradation of pollutants. New Journal of Chemistry, 2020, 44, 12247-12255.	1.4	4
63	Interface engineering in the α-Co(OH) <sub>2</sub> /ZIF-67 heterostructure for enhanced oxygen evolution electrocatalysis. New Journal of Chemistry, 2021, 45, 10199-10203.	1.4	4
64	Synthesis, structure and photoluminescent behavior of a novel pillar-layered {Zn <sub>3</sub> }-based metal–organic framework. Functional Materials Letters, 2016, 09, 1650002.	0.7	3
65	Assembling hierarchical metal–oxygen building units with a semirigid tetracarboxylate ligand into a three-dimensional framework for nitrobenzene sensing. Dalton Transactions, 2017, 46, 6523-6527.	1.6	3
66	Effect of ROS generation on highly dispersed 4-layer O-Ti7O13 nanosheets toward tumor synergistic therapy. Materials Science and Engineering C, 2021, 120, 111666.	3.8	3
67	Surface Structure Engineering of Nanosheet-Assembled NiFe2O4 Fluffy Flowers for Gas Sensing. Nanomaterials, 2021, 11, 297.	1.9	3
68	The TiO2 topotactic transformation assisted trapping of an atomically dispersed Pt catalyst for low temperature CO oxidation. RSC Advances, 2019, 9, 16774-16778.	1.7	2
69	Preparation of 2D ultrathin titanium dioxide nanosheets with enhanced visibleâ€light photocatalytic activity. Micro and Nano Letters, 2021, 16, 313-318.	0.6	2
70	In Situ Growth and Electrochemical Activation of Copper-Based Nickel–Cobalt Hydroxide for High-Performance Energy Storage Devices. ACS Applied Energy Materials, 2021, 4, 9460-9469.	2.5	2
71	Soft X-ray-Enhanced Reactive Oxygen Species Generation in Mesoporous Titanium Peroxide and the Application in Tumor Synergistic Therapy. ACS Applied Bio Materials, 2020, 3, 7408-7417.	2.3	1
72	An Feâ€MIL100 Based Drug Delivery System for pH and Glutathione Dualâ€Responsive Drug Release. ChemistrySelect, 2021, 6, 12295-12299.	0.7	1

#	Article	IF	CITATIONS
73	Plant polyphenol-involved coordination assembly-derived Mo <sub>3</sub> Co <sub>3</sub> C/Mo <sub>2</sub> C/Co@NC with phase regulation and interface engineering for efficient hydrogen evolution reaction electrocatalysis. New Journal of Chemistry, 0, ,	1.4	1